AEROELASTIC EIGENVALUE ANALYSIS OF THREE-BLADED WIND TURBINES

M.H. Hansen
Wind Energy Department
Risø National Laboratory
DK-4000 Roskilde, Denmark
morten.hansen@risoe.dk

Abstract

A method for aeroelastic eigenvalue analysis of three-bladed wind turbines is presented. The method is described in a general form, as independent of the particular aeroelastic modelling as possible. The turbine structure is modelled by a Finite beam Element Method, and the aerodynamic loads are modelled by the Blade Element Momentum method coupled with a Beddoes-Leishman type dynamic stall model in a state-space formulation. The linearization of the equations of motion is performed about a steady-state equilibrium, where the deterministic forcing of the turbine is neglected. To eliminate the periodic coefficients and avoid using the Floquet Theory, the multi-blade transformation is utilized. An eigenvalue problem is formulated and the aeroelastic natural frequencies, damping and mode shapes of operating turbines can thereby be computed for any operation condition. An example shows a good agreement between predicted and measured aeroelastic damping of a stall-regulated 600 kW turbine.

Introduction

A new design tool for performing aeroelastic stability analysis of three-bladed wind turbines is presented. The tool may be the first of its kind that is based on eigenvalue analysis and includes dynamic stall. The tool has also been presented in a similar form within the wind energy community [1]; this paper is meant for the the rotorcraft community and contains some introduction to wind turbine dynamics.

Present research in the wind energy community aims at improving the tools for predicting the aeroelastic stability (damping) of turbines, and the tools for design of control systems. The latter is an important objective in the continuous optimization of wind turbines with active power regulation. The next generation of these turbines will be fitted with control systems that, beside power optimization, also actively alleviate loads and actively suppress aeroelastic instabilities under critical operation conditions. Optimal designs of such control systems depend on a linear aeroelastic stability tool.

An early example of such a linear stability tool called ARLIS was represented by Kirchgäßner [2] at EWEC 1984. The tool was originally developed for rotorcraft applications, but can also be used for analyzing wind turbines, as Kirchgäßner showed for an experimental two-bladed machine. Using Floquet Theory for the stability analysis of turbines, ARLIS was ahead of its time, even though the aerodynamic modelling is based on a quasi-steady assumption.

As the first stall-induced vibrations were observed on commercial wind turbines in the early 90's [3], several tools became available for analyzing stability of wind turbines, besides the aeroelastic codes for conducting traditional time-domain analysis. Most tools are based on a method aimed only at predicting stall-induced vibrations [4], where the aerodynamic damping of a blade vibration is approximated as the work done by the aerodynamic forces on the blade over one period of oscillation. The advantage of this method is that the aerodynamic forces may be computed from a nonlinear model, whereby the amplitude dependency of the aerodynamic damping can be investigated. The nonlinear effects of dynamic stall have been shown to limit the aerodynamic damping as the amplitude increases [4, 5], which is important for load assessments on wind turbines.

The disadvantage of approximating damping from work computations is that the prescribed blade vibration must be known on forehand. Often the structural mode shapes of the blades are used in stability assessments with these tools, based on the assumption that the aeroelastic and structural mode shapes are identical, and that the blades vibrate mainly in their mode shapes when mounted on the turbine. But aeroelastic and structural modes are not identical, especially not in the case of a classical flutter instability. Furthermore, blades do not vibrate in pure blade modes when they operate on the rotor; flapwise and edgewise bending modes may couple in the rotor whirling modes of the turbine [6].

Recently, new stability tools for blade only analysis have been developed [7]. Because there are no periodic coefficients in the aeroelastic equations of motion for a blade rotating without influence from the remaining turbine, these tools are based on eigenvalue analysis, similar to a tool developed by Chaviaropoulos [8]. The main issues in developing the new tools have been the linearization and state-space formulation of the aerodynamic models, which normally are used in nonlinear indicial formulations of existing aeroelastic codes. These issues have been solved, and the solutions form the basis in new stability tools for predicting the modal aeroelastic damping of the entire turbine.

A new stability tool called *HAWCStab* for eigenvalue analysis of three-bladed turbines is presented in this paper. The presentation focuses on the method and less on the detailed modelling. The basic model is similar to that of the aeroelastic turbine code HAWC [9, 10]: A Finite beam Element Method is used for the structure, and the aerodynamic loads are modelled by the Blade Element Momentum method coupled with a Beddoes-Leishman type dynamic stall model. This model of unsteady aerodynamics is reformulated in state-space as a set of ordinary differential equations [11]. The coupled equations of motion are linearized about a steady-state equilibrium, where the deterministic forcing of the turbine is neglected. To eliminate the periodic coefficients and avoid using the Floquet Theory, multi-blade coordinates are used directly in the derivation of these linear equations. An eigenvalue problem is then set up, where the eigenvalues and eigenvectors can be computed at any operation condition to give the aeroelastic natural frequencies, damping and mode shapes of the entire turbine. This approach is presently limited to isentropic rotors (identical blades and uniform inflow), because of the multi-blade transformation. However, it can be extended to handle ground fixed asymmetries, e.g. gravity loads, cyclic pitch, rotor tilt, and yaw errors.

The paper structured as follows: First, the linear aeroelastic model is described with focus on the issues that are important for setting up the eigenvalue problem. Second, the eigenvalue analysis is describing including issues about conditioning the eigenvalue problem and interpretation of the eigensolutions. Finally, a stability analysis is presented for a stall-regulated 600 kW turbine, which has been used in an experiment to estimate the aeroelastic modal damping of its edgewise whirling modes [12]. For readers unfamiliar with wind turbine dynamics, the purely structural modes of this turbine are introduced by a modal analysis similar to [6].

Linear aeroelastic model

The linear aeroelastic model of three-bladed horizontal axis wind turbines used in HAWCStab is described in this section. The turbine is modelled by articulated Timoshenko beam elements using the Finite Element Method, where the aerodynamic forces obtained by a Blade Element Momentum method are transformed to the nodes assuming parabolic distribution over the blade elements. The linear equations of motion are derived using Lagrange's equations in a linear formulation. To enable the eigenvalue analysis, the periodic coefficients in these equations are eliminated by formulating the structural and aerodynamic degrees of freedom (DOFs) for the rotor in *multi-blade coordinates*.

Multi-blade coordinates

The multi-blade transformation, or Coleman transformation for bladed rotors [13, 14] is a method to describe the individual blade coordinates in the ground fixed frame of reference. The periodic terms in governing aeroelastic equations can thereby be eliminated, when the number of rotor blades is odd, the rotor is *isotropic* (identical and symmetrically mounted blades), and the inflow to the rotor is uniform. These conditions can be expanded to ground fixed cyclic variations in blade properties and inflow, e.g. due to tilt and yaw of rotor, or cyclic blade pitch.

The periodic terms are eliminated because all coordinates of the model are defined in the same frame of reference. The wind field and the motion of the tower and nacelle are defined in the ground fixed frame. The bending of the main shaft are defined in the ground fixed frame by a simple rotational transformation of the shaft coordinates with respect to the azimuth angle. A physical coordinate q_k for blade number k, defined in its own co-rotating frame, is transformed into the ground fixed frame by the multi-blade transformation:

$$q_k(t) = a_0(t) + a_1(t)\cos\left(\Omega t + \frac{2\pi}{3}(k-1)\right) + b_1(t)\sin\left(\Omega t + \frac{2\pi}{3}(k-1)\right) \quad (1)$$

where t is time, $k = 1, 2, 3$ is the blade number, and Ω is the mean rotational speed of the rotor. Three multi-blade coordinates a_0, a_1, and b_1 replace the three blade coordinates q_1, q_2, and q_3.

To understand that the multi-blade coordinates describe the rotor coordinates in the ground fixed

frame, assume that blade coordinates q_k describes a flapwise blade deflection. In that case, the a_0 coordinate describes a simultaneous flapwise deflection of all three blades, while the a_1 and b_1 coordinates describe tilt and yaw motions of the rotor, respectively (azimuth angles are measured from the vertical downward position).

Similar considerations can be used for the remaining blade coordinates of both structural and aerodynamic DOFs in an aeroelastic model. The following two sections describes the linear aeroelastic model used for the eigenvalue analysis in HAWCStab, where all blade coordinates are defined in multi-blade coordinates by the transformation (1).

Structural dynamics

The turbine structure is modelled by articulated prismatic beam elements as shown schematically in Figure 1. The beam structures can be divided into three substructures: Tower, nacelle including the shaft, and blades. These substructures are kinematically coupled at the tower top and rotor center nodes.

The tower is assumed to be clamped at the first node of the tower substructure. The tower top node has the same DOFs as the first node of nacelle substructure, except for a *constant* speed azimuthal rotation of the shaft node. In this first version of HAWCStab there is no rotational DOF for modelling the generator. The nacelle substructure models both nacelle deformations and torsional deformations of drive-train, which is rotating at the constant rotor speed. The three blades are connected to the nacelle at the rotor center, whereby the first common blade node has the same DOFs as the shaft end, when accounting for the 120° azimuthal blade rotations.

The Timoshenko beam theory, used for the prismatic beam elements, includes the shear deformations and rotational inertia of the beam cross-sections. Each node has therefore six DOFs: Two pairs of cross-sectional translations and rotations, a longitudinal translation, and a torsional rotation. The shape functions used to describe the variations of these deformations over the element as function of the element coordinate and node DOFs are similar to the functions suggested in [15]. The six deformations of all beam cross-sections of the turbine model is thereby described by the node deformation vector:

$$\mathbf{u} = \{\mathbf{u}_t \ \mathbf{u}_n \ \mathbf{u}_{a_0} \ \mathbf{u}_{a_1} \ \mathbf{u}_{b_1}\}^T \tag{2}$$

where $\mathbf{u}_t$ contains the tower node DOFs, $\mathbf{u}_n$ contains the nacelle node DOFs described in the fixed frame

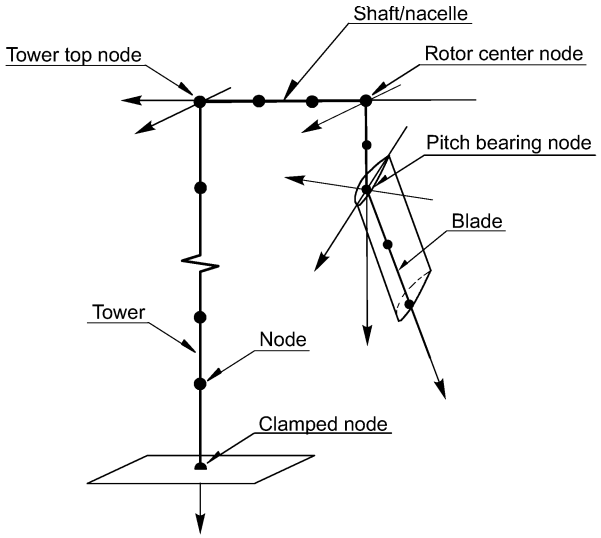

Figure 1: Schematics of the articulated beam element model of a wind turbine used in HAWCStab. Note that only one blade is drawn.

of reference, $\mathbf{u}_{a_0}$ contains the symmetric node DOFs of the rotor blades, and the two vectors $\mathbf{u}_{a_1}$ and $\mathbf{u}_{b_1}$ contain the two asymmetric node DOFs of the rotor blades (cf. equation (1)).

The equations of motion are derived using Lagrange's equation. The total kinetic energy can be written as

$$T = \sum_{k=1}^{N_e} T_k(\mathbf{u}, \dot{\mathbf{u}}) \tag{3}$$

where N_e is the total number of elements, $\dot{\mathbf{u}}$ is the node velocity vector, and T_k is the kinetic energy of element number k, which is derived as

$$T_k(\mathbf{u}, \dot{\mathbf{u}}) = \frac{1}{2}\frac{m_k}{A_k}\int_0^{l_k}\int_A \dot{\mathbf{r}}_k^T \dot{\mathbf{r}}_k \, dA \, dz \tag{4}$$

where $\dot{\mathbf{r}}_k = \dot{\mathbf{r}}_k(x, y, z; \mathbf{u}, \dot{\mathbf{u}})$ is a velocity vector in the ground fixed frame for the cross-sectional mass particle with mass m_k/A_k at cross-sectional position (x, y) and element coordinate z, and l_k, m_k and A_k are the length, mass per unit-length, and area of the cross-section for the prismatic element k. This velocity vector is obtained as the time derivative of the position vector, which is not written out here for the brevity of this paper.

The total potential energy can be written as

$$V = \sum_{k=1}^{N_e} V_k(\mathbf{u}) \tag{5}$$

where V_k is the potential energy stored in element number k, which for rotor elements has the form

$$V_k(\mathbf{u}) = V_{e,k}(\mathbf{u}) + V_{c,k}(\mathbf{u}) \tag{6}$$

where $V_{e,k}$ is the elastic strain energy, and $V_{c,k}$ is the potential energy due to centrifugal blade forces. The geometric nonlinearity that an element is elongated by variations in cross-sectional deformations, causes energy from the centrifugal normal forces to be stored in the blade elements.

It is important to note that the presumption of an isotropic rotor for the use of multi-blade coordinates to eliminate the periodic coefficients in the equations of motion, also implies that the blade nodes are identical for all three rotor blades. Each set of three identical blade elements can therefore be collected to a single *rotor element*, which simplifies the derivation of the equation of motion using Lagrange's equation on element level. The contribution to the Lagrangian $L = T - V$ from a rotor element is the sum of the contributions from the three identical blade elements:

$$L_k^r = T_k^{B_1} + T_k^{B_2} + T_k^{B_3} - V_k^{B_1} - V_k^{B_2} - V_k^{B_3} \tag{7}$$

where the subscript k here refers to the rotor element number. Similar to the contributions from a tower element L_k^t and a nacelle element L_k^n, this collected contribution from a rotor element is independent of time t because of the multi-blade formulation. The element contributions to the Lagrangian depend only on the structural state $L_k = L_k(\mathbf{u}, \dot{\mathbf{u}})$, where the superscripts are omitted.

Lagrange equations including generalized aerodynamic forces can be written as

$$\sum_k \left(\frac{\partial}{\partial t} \left(\frac{\partial L_k}{\partial \dot{u}_i} \right) - \frac{\partial L_k}{\partial u_i} \right) = Q_i \tag{8}$$

where $i = 1, 2, \ldots, N$, the summation over index k includes the tower, nacelle, and rotor elements, and $N = 6 \times N_e$ is the total number of generalized coordinates (DOFs). Note that there is no dissipation function introduced here; structural damping will be added to the equation of motion as element matrices based on a Rayleigh type damping model [16].

Linearization of Lagrange's equations (8) and introduction of structural damping yields that the linear equation of motion can becomes

$$\mathbf{M}\ddot{\mathbf{u}} + (\mathbf{C} + \mathbf{G})\,\dot{\mathbf{u}} + \mathbf{K}\mathbf{u} = \mathbf{Q} \tag{9}$$

where the damping matrix C is derived from the Rayleigh type damping model. Using that the contributions to the Lagrangian from all elements are autonomous, the contributions of element k to the mass, gyroscopic, and stiffness matrices can be derived as

$$\begin{aligned} m_{ij,k} &= \left. \frac{\partial^2 L_k}{\partial \dot{u}_i \partial \dot{u}_j} \right|_{\mathbf{u}=\mathbf{u}_0,\ \dot{\mathbf{u}}=\mathbf{0}} \\ g_{ij,k} &= \left. \left(\frac{\partial^2 L_k}{\partial \dot{u}_i \partial u_j} - \frac{\partial^2 L_k}{\partial u_i \partial \dot{u}_j} \right) \right|_{\mathbf{u}=\mathbf{u}_0,\ \dot{\mathbf{u}}=\mathbf{0}} \\ k_{ij,k} &= \left. - \frac{\partial^2 L_k}{\partial u_i \partial u_j} \right|_{\mathbf{u}=\mathbf{u}_0,\ \dot{\mathbf{u}}=\mathbf{0}} \end{aligned} \tag{10}$$

where $\mathbf{u}_0$ is the steady state deformation of the turbine, which in this first version of HAWCStab is assumed to be a symmetric deformation of the rotor. Note that the mass and stiffness matrices are symmetric, and the gyroscopic matrix is anti-symmetric.

Aerodynamics

The distribution of aerodynamic forces over an blade element is assumed to be parabolic, whereby three aerodynamic calculation points are needed for each element. To reduce the total number of calculation points and ensure that the distribution over the entire blade is continuous, the three calculation points are placed at the nodes and the middle of each element. Because the aerodynamic forces are assumed to vanish at the tip and rotor center, the number of calculation points is $N_{ap} = 2N_{eb} - 1$ for each blade, where N_{eb} is the number of blade elements.

A Beddoes-Leishman type dynamic stall model in a state-space formulation recently developed at Risø National Laboratory [11] is used to model the unsteady forces in each aerodynamic calculation point. The model includes the dynamic effects of the near wake (Theodorsen Theory) and the trailing edge separation in stall on the lift, drag, and moment coefficients. However, the effect of leading edge separation is neglected because of the moderate reduced frequencies and types of airfoils applicable for turbine blades. Added fluid mass is also neglected due to the moderate reduced frequencies.

Figure 2 shows an example of typical loops of the unsteady lift and drag coefficients for vibrations about different angles of attack. The model of the trailing separation is highly nonlinear, however it can be linearized with reasonable agreement between linear and nonlinear loops, even for relatively large variations in angle of attack, as seen in Figure 2.

The model uses four aerodynamic states to describe the dynamics of the unsteady lift, drag, and moment

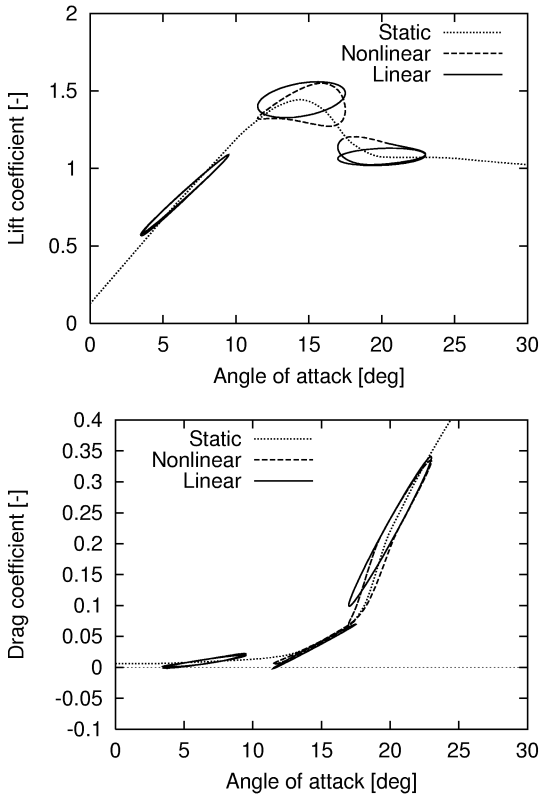

Figure 2: Linear and nonlinear unsteady lift and drag coefficients computed from the Beddoes-Leishman type dynamic stall model developed in a state-space formulation by Hansen et al. [11]. Model parameters and reduced frequencies used in this example are typical for turbine blades.

coefficients [6]: Two states to model the two time-lags in the near wake effect (corresponding to a two time-lag approximation to the indicial function of the Theodorsen theory), and two time-lags in the effect of trailing edge separation (one lag in the pressure distribution over the chord, and one lag in movement in the separation point). Hence, the total number of aerodynamic states is $N_a = 4 \times 3 \times N_{ap}$, which are collected in an aerodynamic state vector:

$$\mathbf{x} = \{\mathbf{x}_{a_0}\ \mathbf{x}_{a_1}\ \mathbf{x}_{b_1}\}^T \tag{11}$$

where $\mathbf{x}_{a_0}$ contains the symmetric aerodynamic states, and the two vectors $\mathbf{x}_{a_1}$ and $\mathbf{x}_{b_1}$ contain the two asymmetric aerodynamic states of the rotor blades, as defined by equation (1).

The linear first order dynamic equations for the aerodynamic states can be written as [11]

$$\dot{\mathbf{x}} + \mathbf{A}_d\,\mathbf{x} = \mathbf{H}(\mathbf{u}, \dot{\mathbf{u}}) \tag{12}$$

where $\mathbf{A}_d$ is a matrix having uncoupled 4×4 matrices in the diagonal, one for each aerodynamic calculation point. The vector on the right hand side is an inherent nonlinear function of the deformation and velocity vectors describing the effect of turbine vibrations on the angle of attack, pitch rates, and relative inflow velocity at the calculation points. This function is linearized as

$$\mathbf{H}(\mathbf{u}, \dot{\mathbf{u}}) \approx \mathbf{C}_{ux}\dot{\mathbf{u}} + \mathbf{K}_{ux}\mathbf{u} \tag{13}$$

The linearization of the dynamic stall model to obtain the matrix $\mathbf{A}_d$ and linear approximation of the function $\mathbf{H}$ is performed about the steady state given by the symmetric deformation $\mathbf{u}_0$ of the rotor and a symmetric aerodynamic state $\mathbf{x}_0$. This steady state is computed simultaneously with the induced velocities to obtain the influence of the wake on the steady state conditions. The wake is assumed to be fixed, i.e., the induced velocities computed for each operational condition are constant and independent of rotor vibrations.

The aerodynamic forces and moments in the calculation points on the blades are given by nonlinear functions of the aerodynamic states $\mathbf{x}$, and the structural states $\mathbf{u}$ and $\dot{\mathbf{u}}$ due to their effect on the angles of attack, pitch rates, and relative inflow velocities. The three calculation points for each blade element enable the derivation of a parabolic distribution of cross-sectional forces and torsional moment over the element k:

$$\mathbf{F}_k = \mathbf{F}_k(z; \mathbf{u}, \dot{\mathbf{u}}, \mathbf{x}) \ \text{ and } \ M_k = M_k(z; \mathbf{u}, \dot{\mathbf{u}}, \mathbf{x}) \tag{14}$$

where z is the element coordinate. These forces (which are not written out here for brevity) are defined in the ground fixed frame, and they are applied in the aerodynamic center of the blade cross-section, resulting in the generalized forces [17]:

$$Q_i = \sum_k \int_0^{l_k} \left(\mathbf{F}_k^T \frac{\partial \mathbf{r}_{AC,k}}{\partial u_i} + M_k \frac{\partial \theta_{AC,k}}{\partial u_i} \right) dz \tag{15}$$

where $i = 1, 2, \ldots, N$, the summation over index k includes all blade elements, the vector $\mathbf{r}_{AC,k} = \mathbf{r}_{AC,k}(z; \mathbf{u})$ describes the position of the aerodynamic center in the ground fixed frame, and $\theta_{AC,k} = \theta_{AC,k}(z; \mathbf{u})$ is the torsion of the cross-section.

After linearization of (15) about the steady state ($\mathbf{u}_0$,$\mathbf{x}_0$), the generalized aerodynamic forces can be approximated by

$$\mathbf{Q}(\mathbf{u}, \dot{\mathbf{u}}, \mathbf{x}) \approx \mathbf{C}_a\dot{\mathbf{u}} + \mathbf{K}_a\mathbf{u} + \mathbf{A}_f\mathbf{x} \tag{16}$$

where the contribution to the aerodynamic damping and stiffness matrices ($\mathbf{C}_a$ and $\mathbf{K}_a$) and the coupling

matrix $\mathbf{A}_f$ from each blade element is derived as

$$
\begin{aligned}
c_{a,ij,k} &= \int_0^{l_k} \left(\frac{\partial \mathbf{F}_k^T}{\partial \dot{u}_j} \frac{\partial \mathbf{r}_{AC,k}}{\partial u_i} + \frac{\partial M_k}{\partial \dot{u}_j} \frac{\partial \theta_{AC,k}}{\partial u_i} \right) \Big|_0 dz \\
k_{a,ij,k} &= \int_0^{l_k} \left(\frac{\partial \mathbf{F}_k^T}{\partial u_j} \frac{\partial \mathbf{r}_{AC,k}}{\partial u_i} + \frac{\partial M_k}{\partial u_j} \frac{\partial \theta_{AC,k}}{\partial u_i} \right. \\
&\qquad \left. + \mathbf{F}_{0,k}^T \frac{\partial \mathbf{r}_{AC,k}}{\partial u_i \partial u_j} + M_{0,k} \frac{\partial \theta_{AC,k}}{\partial u_i \partial u_j} \right) \Big|_0 dz \\
a_{f,ij,k} &= \int_0^{l_k} \left(\frac{\partial \mathbf{F}_k^T}{\partial x_j} \frac{\partial \mathbf{r}_{AC,k}}{\partial u_i} + \frac{\partial M_k}{\partial x_j} \frac{\partial \theta_{AC,k}}{\partial u_i} \right) \Big|_0 dz
\end{aligned}
\tag{17}
$$

where $\mathbf{F}_{0,k}$ and $M_{0,k}$ are the steady state force and moment distributions for element k, and all expressions are evaluated at $(\mathbf{u}, \dot{\mathbf{u}}, \mathbf{x}) = (\mathbf{u}_0, \mathbf{0}, \mathbf{x}_0)$. These matrix contributions do not have any type of symmetry, which corresponds to the fact that the aerodynamic forces $\mathbf{Q}$ are circulatory.

Collection of equations (9), (12), (13), and (16) yields the coupled equations of motion of the linear aeroelastic model of wind turbines:

$$
\begin{aligned}
\mathbf{M}\ddot{\mathbf{u}} + (\mathbf{C} + \mathbf{G} + \mathbf{C}_a)\,\dot{\mathbf{u}} & \\
+ (\mathbf{K} + \mathbf{K}_a)\,\mathbf{u} + \mathbf{A}_f \mathbf{x} &= 0 \\
\dot{\mathbf{x}} + \mathbf{A}_d\,\mathbf{x} + \mathbf{C}_{ux}\dot{\mathbf{u}} + \mathbf{K}_{ux}\mathbf{u} &= 0
\end{aligned}
\tag{18}
$$

These equations are autonomous enabling an eigenvalue analysis to determine the aeroelastic natural frequencies, damping, and mode shapes of wind turbines operating at a constant rotor speed.

Eigenvalue Analysis

The aeroelastic equations of motion (18) couple the structural motion of the turbine with the dynamics of the aerodynamic forces. The structural dynamics is characterized by N natural modes with frequencies and damping through a second order differential equation, whereas the dynamics described by the independent first order differential equation for each aerodynamic calculation point can be characterized as over-damped aerodynamic states.

The coupling of dynamic and purely damped states means that a direct formulation of an eigenvalue problem from (18) will lead to an ill-conditioned problem. This issue cannot be solved but the problem can be better conditioned by a modal expansion of the structural DOFs. The undamped eigenvectors of the stationary turbine $\mathbf{v}_i$ (computed from the mass and stiffness matrix of the turbine at standstill) are used for this exapnsion:

$$
\mathbf{u} = \sum_{i=1}^{N} \mathbf{v}_i\, z_i(t) = \mathbf{\Phi}\,\mathbf{z} \tag{19}
$$

where $\mathbf{\Phi}$ is a modal matrix containing the undamped eigenvectors in the columns, and $\mathbf{z}$ is a new structural state vector.

To set up the eigenvalue problem all aeroelastic states are collected in a single state vector

$$
\mathbf{y} = \begin{Bmatrix} \mathbf{x} \\ \mathbf{z} \\ \dot{\mathbf{z}} \end{Bmatrix} \tag{20}
$$

and a solution of the form $\mathbf{y} = \mathbf{w}e^{\lambda t}$ is sought. After use of expansion (19) and insertion of this solution form, the following eigenvalue problem is obtained

$$
\left(\begin{bmatrix} \mathbf{A}_d & \mathbf{K}_{ux}\mathbf{\Phi} & \mathbf{C}_{ux}\mathbf{\Phi} \\ \mathbf{0} & \mathbf{0} & -\mathbf{I} \\ \mathbf{\Phi}^T\mathbf{A}_f & \mathbf{\Phi}^T\mathbf{K}_t\mathbf{\Phi} & \mathbf{\Phi}^T\mathbf{C}_t\mathbf{\Phi} \end{bmatrix} + \lambda \mathbf{I} \right) \mathbf{w} = \mathbf{0} \tag{21}
$$

where $\mathbf{K}_t = \mathbf{K} + \mathbf{K}_a$ and $\mathbf{C}_t = \mathbf{C} + \mathbf{G} + \mathbf{C}_a$ are the total stiffness and damping matrices. The eigenvalues λ_n and eigenvectors $\mathbf{w}_n$ of this problem yields the natural frequencies, damping, and mode shapes of the aeroelastic turbine modes.

Natural frequency and logarithmic decrement of mode n are given by the imaginary and real part of the corresponding eigenvalue $\lambda_n = \sigma_n + i\omega_n$ as

$$
f_n = \frac{\omega_n}{2\pi} \qquad \text{and} \qquad \delta_n = -\frac{\sigma_n}{f_n} \tag{22}
$$

and the corresponding mode shape can be computed in physical (blade) coordinates from the eigenvector $\mathbf{w}_n$ by the modal expansion (19) and the multi-blade transformation (1). This computation of modal amplitudes for the physical blade coordinates enables an identification of the modes as described in [6].

Identification of modes

Insertion of the solution $\mathbf{y} = \mathbf{w}_n e^{\lambda_n t}$ into (19), the modal solution for the multi-blade coordinates of a particular rotor element DOF can be written as

$$
\begin{Bmatrix} a_0(t) \\ a_1(t) \\ b_1(t) \end{Bmatrix} = \mathrm{Re}\left\{ \begin{Bmatrix} a_{0,n} \\ a_{1,n} \\ b_{1,n} \end{Bmatrix} e^{\lambda_n t} \right\} \tag{23}
$$

where the complex modal amplitudes $a_{0,n}$, $a_{1,n}$, and $b_{1,n}$ is given by $\mathbf{w}_n$ and $\mathbf{\Phi}$. Insertion of these multi-blade coordinates into the transformation (1) yields

that the modal solution for the physical DOF $q_{k,n}$ on blade number k vibrating in mode n becomes

$$\begin{aligned} q_{k,n} &= A_n^0 e^{\sigma_k t}\cos(\omega_n t + \phi_n^0) \\ &+ \tfrac{1}{2}A_n^{\mathrm{BW}} e^{\sigma_k t}\cos\Big((\omega_n+\Omega)t + \tfrac{2\pi}{3}(k-1) + \phi_n^{\mathrm{BW}}\Big) \\ &+ \tfrac{1}{2}A_n^{\mathrm{FW}} e^{\sigma_k t}\cos\Big((\omega_n-\Omega)t - \tfrac{2\pi}{3}(k-1) + \phi_n^{\mathrm{FW}}\Big) \end{aligned} \quad (24)$$

where the amplitudes $(A_n^0, A_n^{\mathrm{BW}}, A_n^{\mathrm{FW}})$ and phases $(\phi_n^0, \phi_n^{\mathrm{BW}}, \phi_n^{\mathrm{FW}})$ are uniquely determined by the complex modal amplitudes $a_{0,n}$, $a_{1,n}$, and $b_{1,n}$.

Equation (24) shows that for turbine vibrations in mode n, the motion of blade number k in the particular physical coordinate $q_{k,n}$ consists of three components: A symmetric component where all blades deflect simultaneously with the amplitude $A_{k,n}^0$, and two asymmetric components where the blades deflect with phase shifts of $2\pi/3$ and the amplitudes $A_{k,n}^{\mathrm{BW}}$ and $A_{k,n}^{\mathrm{FW}}$, respectively. As indicated by the superscripts, the asymmetric components represent *backward* and *forward rotor whirling*. The direction of the whirl is determined by sign of the blade dependent phase shifts $\frac{2\pi}{3}(i-1)$.

The frequency of the symmetric component is ω_k while the frequencies of the backward and forward blade whirl components are $\omega_k + \Omega$ and $\omega_k - \Omega$, respectively. The reason for these frequency shifts is that the natural frequency ω_k is given in the ground fixed frame. An observer on the tower top (in the ground fixed frame) will measure the natural frequency ω_k, however the observer on a blade will measure the frequencies $\omega_k+\Omega$ and $\omega_k-\Omega$ for a backward and forward whirling modes, respectively.

Often, the asymmetric rotor modes of a turbine are not purely forward, or backward whirling, but consists of both forward and backward whirling components, and some symmetric component. In such cases, the observer on the blade will see three peaks for each mode in the frequency response.

Note that the exponential decay (or growth in case of instability) of blade amplitudes given by $e^{\sigma_n t}$ is independent of the reference frame of the observer.

As the following example will show, it is possible to identify the symmetric and asymmetric rotor modes of a turbine by computing the symmetric and whirling components for the DOFs at the blade tip nodes of the rotor. To identify the tower bending modes it may be necessary to compute the modal amplitudes for the tower top DOFs.

Prediction compared to observation

Thomsen *et al.* [12] have developed an experimental method for estimating the aeroelastic damping of turbine modes while the turbine is operating. In their experiment with a stall-regulated 600 kW Bonus turbine, the low damping of the two first edgewise whirling modes were estimated. They showed that the forward whirling mode is more damped than the backward whirling mode, although they are associated with the same edgewise blade mode.

Hansen [6] presented a theoretical modal analysis of the particular turbine based on a simplified turbine model, which showed that the blades vibrated more out of the rotor plane in the forward whirling than in the backward whirling mode. This difference can explain the measured difference in aerodynamic damping of the two modes because out of plane blade vibrations are more damped than in plane vibrations.

In this section the aeroelastic modes are computed with HAWCStab for the same 600 kW turbine. The results support the conclusion by Hansen [6], and also shows that the predicted aeroelastic damping of the two turbine modes correspond well with the observations. For readers unfamiliar with wind turbine dynamics, the modal analysis with the simpler turbine model presented in [6], is redone here based on the more detailed model of HAWCStab.

The input to aeroelastic model is taken from the original HAWC model of the turbine used in the preparations for the experiment by Thomsen *et al.* [12], except for an improved calibration of structural stiffnesses to give the measured frequencies of the first ten structural modes at standstill. These modelled and measured frequencies of the stationary turbine are listed in Table 1. Note that there has only been estimated a single frequency for each of the higher asymmetric mode pairs.

Structural modal analysis

A comparison of modelled and measured frequencies (cf. Table 1) leads to the assumption that the model is sufficiently tuned to the experimental turbine. The naming of the first ten modes is based on animations of their mode shapes and the measured frequency responses. The sequence of modes is typical for a turbine of this size; with the exception that the 1st shaft torsion mode may be higher than the tower bending modes. The longitudinal tower bending lies always slightly lower than the lateral tower bending mode because it contains some tilting of the rotor which has a large inertia.

Mode no.	Mode name	Modelled freq. [Hz]	Measured freq. [Hz]
1	1st shaft torsion	0.55	0.56
2	1st long. tower	0.76	0.73
3	1st lat. tower	0.81	0.80
4	1st yawing flap	1.41	1.2
5	1st tilting flap	1.50	1.5
6	1st sym. flap	1.70	1.76
7	1st vertical lag	2.92	2.9
8	1st horizontal lag	2.99	
9	2nd yawing flap	3.43	3.6
10	2nd tilting flap	3.64	

Table 1: Modelled and measured natural frequencies of the lowest 10 modes of the stationary turbine.

Modes 4 and 5 are the 1st tilt/yaw modes involving the first flapwise blade mode. The yaw mode most often lies lower than the tilt mode because towers are stiffer in tilt than in yaw. The sixth mode is the 1st symmetrical flap mode, where the blades vibrate simultaneously in the flapwise blade mode in counter phase with a longitudinal tower vibration.

Modes 7 and 8 involve the first edgewise blade mode and their frequencies are close to the edgewise blade frequency of 2.94 Hz. In both modes, the blades vibrate edgewise against each other so that they cancel out the torsional moment at the rotor center. The two modes differ in the direction of the reactive force at the rotor center, as indicated by their names: 1st vertical and 1st horizontal edgewise mode. The sequence of these two modes is given by the vertical and horizontal stiffness of the rotor support.

Modes 9 and 10 are the 2nd tilt/yaw modes, where the rotor blades are tilting and yawing in counter phase with the tilt and yaw of the nacelle. Again the yaw mode lies below the tilt mode because of the lower yaw than tilt stiffness of the tower.

Figure 3 shows how the natural frequencies and structural damping of these first ten modes change with the rotation speed of the rotor, from standstill to the operation speed. The frequencies of the tower bending modes and the shaft torsion mode are constant with rotor speed. The frequency of the symmetric flap mode increases due to centrifugal stiffening of flapwise bending. The frequencies of the asymmetric rotor modes change with the rotor speed due to gyroscopic effects.

All pairs of asymmetric rotor modes at standstill (modes 4/5, modes 7/8, and modes 9/10) become pairs of rotor whirling modes due to the rotation,

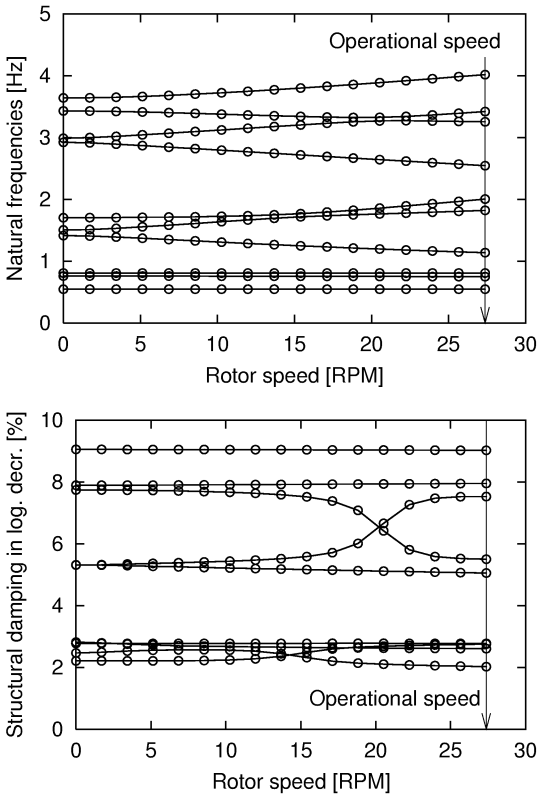

Figure 3: Campbell diagram (top) and damping diagram (bottom) showing the natural frequencies and structural damping of the first ten structural turbine modes versus the rotation speed of the rotor.

e.g. the 1st tilt/yaw modes become the *1st flapwise whirling modes* and the 1st pair of edgewise modes become the *1st edgewise whirling modes*. The frequencies of the backward whirling (BW) modes decrease with rotor speed, whereas the frequencies of the forward whirling (FW) modes increase with rotor speed.

The damping diagram in Figure 3 shows the structural damping of the first ten modes as modelled by the Rayleigh type damping model. The levels of the damping are assumed from experience, noting that the blades are fitted with edgewise vibration dampers, yielding damping of approximately 5 % logarithmic decrement for the first edgewise blade mode, whereby the first edgewise whirling mode pair obtain about the same level of damping (see Figure 6). The damping of the 1st shaft torsion mode is not included in Figure 3, because this damping is difficult to model without the modelling of the induction generator. Note that some modes seems to interchange levels of damping, which is due to the modal interactions discussed in the following.

The splitting of the natural frequencies of a whirling mode pair with the rotor speed Ω is related to the coordinate system of observation through gyroscopic effects. The natural frequencies ω_n in Figure 3 are observed from the ground fixed frame. Equation (24) shows that in a co-rotating blade frame the frequency of a symmetric rotor mode remains ω_n, whereas the frequencies of BW and FW modes become $\omega_n+\Omega$ and $\omega_n - \Omega$, respectively. If only a single blade mode is involved in a pair of whirling modes, their frequencies will split in the ground fixed frame about the natural frequency ω_{blade} of this blade mode. In this ideal case, the observer on the blade will measure the same frequency $\omega_{\text{blade}} = \omega_n^{\text{BW}} + \Omega = \omega_n^{\text{FW}} - \Omega$ for both the BW and FW mode.

This ideal condition is affected by structural asymmetry of the turbine and coupling of blade modes in the turbine modes. Such modal interactions may occur when the natural frequencies of two turbine modes come close. Figure 3 shows that the frequencies of the 1st FW edgewise mode (mode 8) and the 2nd BW flapwise mode (mode 9) become close at about 20 RPM. These two modes interact, which can be shown by the flapwise and edgewise whirling components in their mode shapes.

Figure 4 shows the FW and BW components of flapwise and edgewise blade motion in modes 7–10. These whirling components are computed from the eigenvectors in multi-blade coordinates as defined in equation (24). The dominating amplitudes for mode 7 and 10 show that these modes are, respectively, a BW edgewise and a FW flapwise mode. However, there are no dominant modal amplitude for modes 8 and 9 over the whole range of rotation speeds. It seems that these modes interchange mode shapes: Mode 8 can be defined as a FW edgewise mode and mode 9 as a BW flapwise mode at rotation speeds below 20 RPM, and above it is vice versa. This modal interaction also explains the interchange of structural damping seen in Figure 3.

At the operation speed, mode 9 must be characterized as the 1st FW edgewise mode with some content of flapwise whirling. Comparison of the flapwise whirling components of modes 7 and 9 shows, what is also shown in [6], that the 1st FW edgewise mode involves more flapwise blade motion than the 1st BW edgewise mode. Hansen [6] suggests that this out of rotor plane motion of the blades can explain the difference in aerodynamic damping of the BW and FW edgewise modes (modes 7 and 9) measured by Thomsen *et al.* [12], and predicted in the following eigenvalue analysis with HAWCStab.

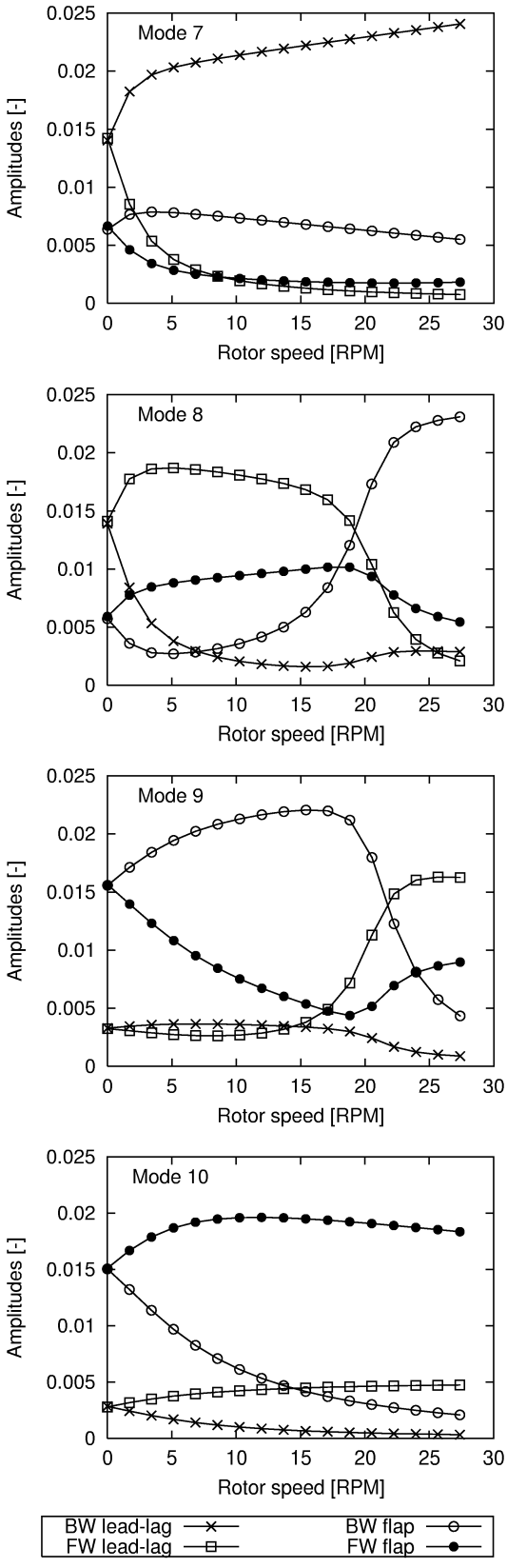

Figure 4: Flapwise and edgewise whirling components of the modal blade amplitudes for modes 7–10 computed as defined in equation (24).

Aeroelastic eigenvalue analysis

Figure 5 shows the structural and aeroelastic natural frequencies and damping of the first ten modes of the turbine operating at different wind speeds (and the operational rotor speed of approx. 27.4 RPM). It shows that the natural frequencies are not affected significantly by the aerodynamic forces, except for the modes involving flapwise blade modes, which are also the most highly damped modes seen in the damping diagram. The lowest and negatively damped mode is the symmetric edgewise (first shaft torsion) mode because of the blade vibrations purely in the rotor plane. On the actual turbine, this mode will be damped by the drive-train damping due to the slip of the induction generator.

The two next lowest damped modes are the two asymmetric edgewise modes, i.e., the forward and backward edgewise whirling modes. Figure 6 shows the predicted and measured aeroelastic damping of these two modes, together with the structural damping for comparison. Although the standard deviations of the measured damping is relatively large, it is clear that these modes have different aeroelastic damping. The same qualitative difference is seen in the predicted aeroelastic damping, and furthermore the level of damping is very similar to the observed damping. These first results with the new tool for stability analysis indicate that it is possible to predict the qualitative and quantitative behavior of the damping of aeroelastic turbine modes.

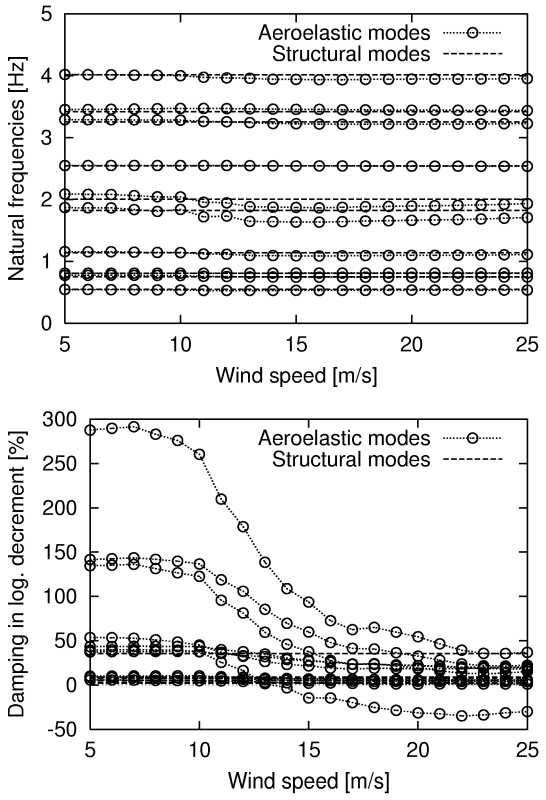

Figure 5: Natural frequencies (top) and damping (bottom) for the first ten structural and aeroelastic modes of the Bonus 600 kW, predicted with HAWCStab for different operation wind speeds.

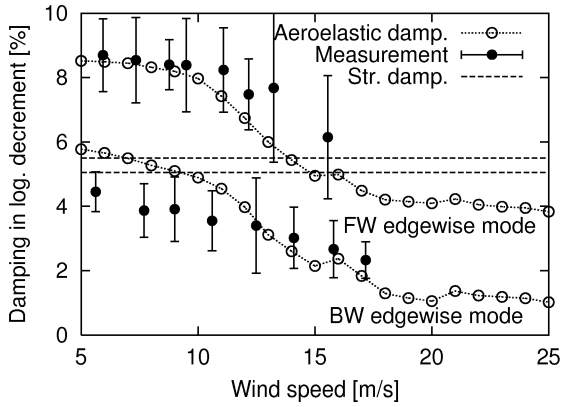

Figure 6: Predicted and measured aeroelastic damping of the forward and backward edgewise whirling modes of the Bonus 600 kW turbine, together with the structural damping to show the change in damping due to the interaction with aerodynamic forces.

Conclusion

In this paper a design tool, called HAWCStab, for performing aeroelastic stability analysis of three-bladed wind turbines is presented. The aeroelastic turbine model is derived from a Finite beam Element Method and the Blade Element Momentum method, where the unsteady aerodynamic forces are modelled by a Beddoes-Leishman type dynamic stall model in a state-space formulation. Multi-blade coordinates are used directly in the derivation of the linear aeroelastic equations of motion to eliminate the periodic coefficients, thereby avoiding the use of Floquet Theory. The eigenvalue problem based on these autonomous equations is ill-conditioned, however the it is conditioned by a modal expansion of the structural degrees of freedom based on the undamped modes of the turbine at standstill. This enables the computation of the natural frequencies, logarithmic decrements, and mode shapes of the aeroelastic turbine modes. An example shows a good agreement between predicted and measured aeroelastic damping of a stall-regulated Bonus 600 kW turbine.

Acknowledgements

This work was partly funded by the European Commission under ENK5–CT–2002–00627 which is gratefully acknowledged.

References

[1] M. H. Hansen. Aeroelastic stability analysis of wind turbines using an eigenvalue approach. In *Proceedings of the European Wind Energy Conference*, Madrid, Spain, June 2003. (In Press).

[2] B. Kirchgäßner. ARLIS – A program system for aeroelastic analysis of rotating linear systems. In W. Palz, editor, *Proceedings of the European Wind Energy Conference 1984*, pages 253–264, Hamburg, Germany, October 1984.

[3] H. Stiesdal. Extreme wind loads on stall regulated wind turbines. In G. Elliot, editor, *Proceedings of the 16th British Wind Energy Association Conference*, pages 101–106, June 1994.

[4] J.T. Petersen, H.Aa. Madsen, A. Björck, P. Enevoldsen, S. Øye, H. Ganander, and D. Winkelaar. Prediction of dynamic loads and induced vibrations in stall. Technical Report Risø-R-1045(EN), Risø, Roskilde, Denmark, May 1998.

[5] F. Rasmussen, J. T. Petersen, and H. Aa. Madsen. Dynamic stall and aerodynamic damping. *ASME Journal of Solar Energy Engineering*, 121:150–155, 1999.

[6] M.H. Hansen. Improved modal dynamics of wind turbines to avoid stall-induced vibrations. *Wind Energy*, 6:179–195, 2003.

[7] P. Chaviaropoulos, E.S. Politis, N.N. Sørensen, M.H. Hansen, B.H. Bulder, D. Winkelaar, D.A. Saravanos, T. Philippidis, C. Galiotis, M.O. Hansen, and T. Kossivas. Recent advances on damped wind turbine rotor blades, the DAMPBLADE project. In *Proceedings of the European Wind Energy Conference 2003*, Madrid, Spain, June 2003. (to appear).

[8] P. K. Chaviaropoulos. Flap/lead-lag aeroelastic stability of wind turbine blades. *Wind Energy*, 4(4):183–200, 2001.

[9] J. T. Petersen. *Kinematically Nonlinear Finite Element Model of a Horizontal Axis Wind Turbine*. PhD thesis, Risø National Laboratory, DK-4000 Roskilde, Denmark, 1990.

[10] J.T. Petersen. The aeroelastic code HawC – model and comparisons. In B. M. Pedersen, editor, *State of the Art of Aeroelastic Codes for Wind Turbine Calculations*, volume Annex XI, pages 129–135, Lyngby, April 1996. International Energy Agency, Technical University of Denmark.

[11] M. H. Hansen, M. Gaunaa, and H. Aa. Madsen. A Beddoes-Leishman type dynamic stall model in state-space and indicial formulations. Technical Report Risø–R–1354(EN), Risø National Laboratory, 2003. (to appear).

[12] K. Thomsen, J. T. Petersen, E. Nim, S. Øye, and B. Petersen. A method for determination of damping for edgewise blade vibrations. *Wind Energy*, 3:233–246, 2001.

[13] W. Johnson. *Helicopter Theory*. Princeton University Press, New Jersey, 1980.

[14] D. A. Peters. Fast floquet theory and trim for multi-bladed rotorcraft. *Journal of the American Helicopter Society*, 39(4):82–89, 1994.

[15] A. Bazoune and Y.A. Khulief. Shape functions of three-dimensional Timoshenko beam element. *Journal of Sound and Vibration*, 259(2):473–480, 2003.

[16] M. H. Hansen. Anisotropic damping of Timoshenko beam elements. Technical Report Risø–R–1267(EN), Risø National Laboratory, 2001.

[17] J. T. Thomsen. *Vibration and Stability, Order and Chaos*. McGraw-Hill, 1997.